Smart rope technology for aquaculture farms - low-cost conductive yarns as load and strain sensors for integrity monitoring

Krish Thiagarajan
Department of Mechanical & Industrial Engineering
University of Massachusetts
Amherst, USA
ORCID:0000-0001-5901-5136

Samer Saleh
Department of Mechanical & Industrial Engineering
University of Massachusetts
Amherst, USA
samersaleh@umass.edu

Nicholas Rotker
Advanced Maritime & Acoustic Technologies Dept.
MITRE
Bedford, USA
nrotker@mitre.org

Margo Lindblom
Advanced Maritime & Acoustic Technologies Dept.
MITRE
Bedford, USA
mlindblom@mitre.org

Cecelia Kane
Advanced Maritime & Acoustic Technologies Dept.
MITRE
Bedford, USA
ckane@mitre.org

James Owens
Nautilus Defense
Pawtucket, RI USA
jim@nautilusdefense.com

***Abstract*—Blue Economy systems like marine energy and aquaculture farms consist of several individual units held by lines made of nylon or fiber ropes. Condition-monitoring of ropes and mooring lines are essential for the overall integrity of a marine energy farm. Our research is aimed at developing a low-cost prototype of a sensor integrated rope that can be used in long-term deployment for comprehensive monitoring purposes. A functional braided composite yarn with integrated electromagnetic properties was integrated into a 5 mm polypropylene rope. Samples with different conductor and core configurations were manufactured by Nautilus Defense. Data processing algorithms for receiving and processing information from the sensors were custom-made and tested at MITRE electronic laboratories. Mechanical tests were conducted at the Ocean Resources and Renewable Energy (ORRE) laboratory at UMass Amherst, where rope samples were subject to varying levels of static and dynamic forcing in dry conditions and under water. The observed linear trend of capacitance with strain offers strong potential for the sensor to support condition monitoring efforts of mooring lines for aquaculture and marine renewable energy.**

Keywords—smart ropes, condition monitoring, mooring lines, capacitance measurement, aquaculture.

I. Introduction

Forecasts by the United Nations suggest that aquaculture will account for 54 percent of the total production of aquatic animals and 60 percent of total aquatic food for human consumption [1]. Due to increases in worldwide demand and limited coastal space, both the aquaculture and fishing industries are moving into the open ocean, where monitoring of equipment as well as health monitoring of the stock become challenging. Compounding this situation are climate change induced factors that result in extreme weather and accelerated wear and tear in equipment, fishing and mooring gear. Blue Economy systems like marine energy and aquaculture farms consist of several individual units held by mooring lines made of nylon or fiber ropes. The lines are secured by anchors embedded onto the seabed. To minimize potential risks for both the marine environment and the operators, intelligent sensors have been employed to provide constant monitoring of environment conditions and equipment performance. Condition-monitoring of rope and mooring lines are essential for the overall integrity of a marine energy farm. Two main approaches specifically employed for fiber ropes include embedded (detectable magnetic threads, optical fibers, conductive threads) and non-embedded (thermography, computer vision, computed tomography, capacitive detection, acoustic emission, and lasers for width measurements) [2]. Currently available as commercial sensors for this purpose include the Rope Measurement System (using system of cameras to measure the rope's cross-section) and the Semi-Autonomous Mooring Inspection Robot (via magnetic flux leakage technique to determine the defects). While embedded sensors are more desirable due to their low cost and less technological set up for end users, it has been a major challenge to integrate the sensor without affecting the material structures/properties [3]. Furthermore, sensors embedded in ropes have high failure rates, or end up costing more to ensure robustness. Our research is aimed at developing a low-cost prototype of a sensor integrated rope that can be used in long-term deployment for comprehensive monitoring purposes.

II. Materials and Methods

A functional braided composite yarn with integrated electromagnetic properties, originally developed for military applications by Nautilus Defense, was integrated into a 5 mm polypropylene rope as a scaled prototype of a smart mooring line

XXX-X-XXXX-XXXX-X/XX/$XX.00 ©20XX IEEE

(Fig. 1). Samples with different conductor and core configurations were manufactured. A core made of twisted yarns/sub rope is labeled as dynamic (Fig. 2), while continuous straight filament bundles form a static core. The layout of the core alters the performance of a rope.

Developed and manufactured by Nautilus Defense, the functional braided composite yarns are comprised of continuous filament polyester yarns and insulated 40-micron-diameter conductors. By incorporating two of these functional braided composite yarns adjacent two each other in the braid's sheath such that they are following offset helical paths, the mutual capacitance between these functional yarns will change based on the rope's kinematics and dynamic behavior under strain. The braid design, conductor content, relative conductor positions, and dielectric properties of both the materials used in the construction of the rope and present in the environment the rope is operating, principally air or water, all have an impact on its capacitive response under strain.

The capacitance between two wires may be given by [4]

$$\mathbb{C} = \frac{2\pi l \epsilon_0 \epsilon_r}{\cosh^{-1}\left(\frac{s^2 - r_{w1}^2 - r_{w2}^2}{2 r_{w1} r_{w2}}\right)} \qquad \text{Eq. (1)}$$

Here l is the length of the wires, ϵ_0 the permittivity of the space between the wires, ϵ_r is the relative permittivity of the wire with respect to the medium, s the distance between the wires, and r_{w1}, r_{w2} are the radii of the two wires. For our analysis, the above model can be modified to account for variation in material between the conductor strands at different tensions. For example, at its minimum tension a submerged rope would be saturated with water between the fibers. If the rope were to be extended then at a theoretical maximum tension, the material between the wires would be mostly rope, as the interstitial water would be squeezed out. Since the emissivity of water is much larger than that of the rope fiber ($\epsilon_r < 1$), the capacitance would decrease with increasing tension. Whereas in dry condition, the reverse occurs because of low emissivity of air.

The data collection hardware is comprised of a microcontroller and a capacitance to digital converter, powered by a battery in a small, watertight tube. A connecter is attached to the copper strands within the wire, and this plugged into the end of the container, connecting internally to the capacitance to digital converter. The capacitance data can be read real time over a serial connection to the microcontroller or logged to an SD card for remote testing and post-processing.

Figure 1. Nautilus-developed capacitive strain-sensing rope

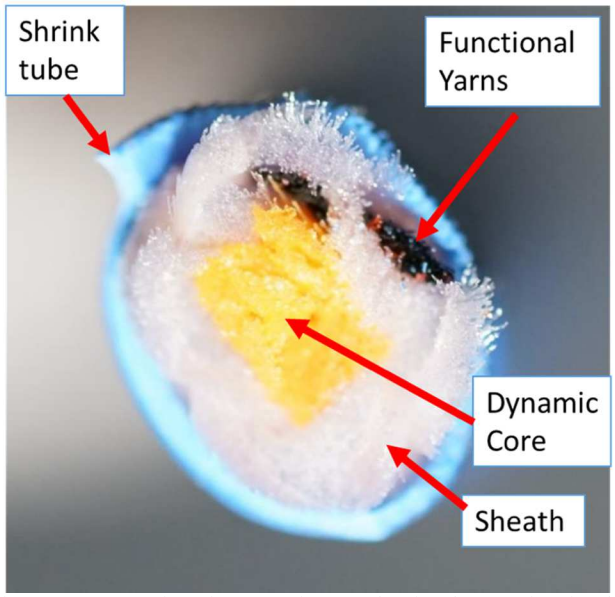

Figure 2. Cross-section of a composite yarn showing the core, functional yarn, sheath and shrink tube.

III. Experimental Campaign

Mechanical tests were conducted at the Structures Laboratory, Department of Civil and Environmental Engineering, and at the Ocean Resources and Renewable Energy (ORRE) laboratory at UMass Amherst. Dry and presoaked samples were tested using an Instron 3369 machine in the Structures Workshop to measure the breaking load. Our preliminary sizing calculations indicated that a 5 mm dry polypropylene rope may have a Minimum Breaking Load (MBL) of 2.64 kN. We were not aware of a procedure for calculating the value for the wet condition.

The 3369 dual column tabletop testing machine is formed of a load frame with integral controller and a jog control panel, a load cell, a set of manually operated grips and Instron Bluehill® test control software. The procedure followed by this study followed the procedure recommended by the American Bureau of Shipping [5], derived from CI standard 1500-02 and listed below:

i. A cycling tension between 1% and 50% of the estimated MBL should be applied 10 times at a period of 12 – 35 sec.

ii. On the last cycle, the rope is pulled to failure, at a loading rate of approximately 20% MBL per minute.

iii. The breaking force (maximum force applied to the rope) and the location of failure are recorded.

In addition, it is recommended by [5] that a minimum length of 40D (D-diameter) be used for MBL estimation, and samples should be soaked in fresh water for 4 hours before testing. Samples of effective length ranging between 210 – 270 mm were tested in both dry and presoaked conditions to failure in order to ascertain the mean breaking load. Fig. 3 shows the force vs. displacement of one sample during the testing. Hysteresis is seen clearly during the process of cyclical loading, which is due to the viscoelastic nature of the rope material. The breaking load

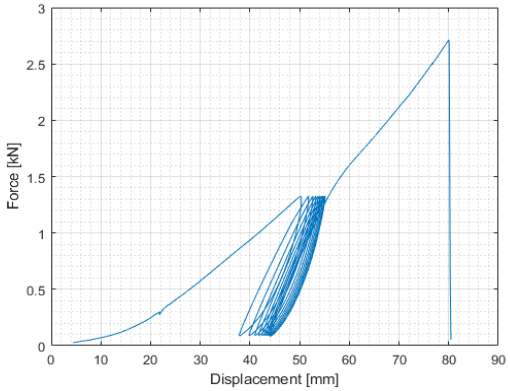

Figure 3. Force vs. displacement showing the breaking point

for this sample was approximately at 2.7 kN. The measured MBL values of all the samples were in the range of 1.9 – 2.7 kN in reasonable agreement with the calculated value.

At the ORRE Wave – Current laboratory, rope samples were subject to varying levels of static and dynamic forcing in dry conditions and under water (Fig. 4). The ORRE facility can generate waves and currents simultaneously, however these capabilities were not utilized here. The facility is equipped with a two-degrees-of-freedom traverse system, which allows for controlled lateral motion of a point of interest along the tank, as well as oscillatory motions in vertical and horizontal directions. The motions can be up to 200 mm amplitude at 2.5 Hz in the horizontal and 100 mm at 2 Hz in the vertical direction. For the purpose of these experiments, quasi-static tests were performed, where the samples were subject to systematic extension and relaxation, while the line tension was measured with a load cell and correlated with the sensor capacitance. Axial loads were recorded using a submersible Kistler 9306A six-axis piezoelectric force and torque sensor. The load cell allows for setting dynamic range, which provides good resolution over the range of expected loads for each run. Outputs were directed through two charge amplifiers and acquired through a NI-9201 voltage input module connected to the CompactRIO-9047. The displacement of the moving end of the sample was recorded directly from the servomotor encoders of the traverse system.

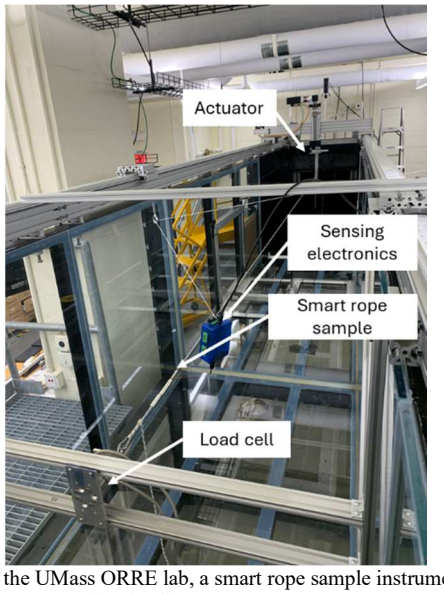

Figure 4. At the UMass ORRE lab, a smart rope sample instrumented with sensing electronics and load cell;

IV. Results and Discussion

Tests were performed on different samples to measure the capacitance vs. displacement in the dry and wet conditions by extending and relaxing gradually while measuring the capacitance. The original condition for the sample was 1% MBL (corresponding to 26.4 N). The samples were extended at a uniform rate of 0.2 mm/sec for short samples and 0.5 mm/sec for long samples until a maximum extension (corresponding to a maximum limit of the actuator, which is 440 N, equivalent to 16.6% MBL) is reached. The load was then progressively decreased until the original condition is reached.

In the following section results from both dry and wet conditions are presented for one sample labeled V1D - Long1 - 117.1 pF - Serial#3) in non-dimensional form. The non-dimensional analysis was performed according to the following steps:

- All plots and variables start from the pretension (1% MBL, corresponding to 26.4 N)
- Strain = (Disp. (i) – Disp. (26.4N))/L0
  - For short samples: L0 = 2000 mm
  - For Long samples: L0 = 6000 mm
- Normalized Cap. = (Cap(i) – Cap (26.4 N))/Max. Cap.
  - In Dry: Max. Cap. = Cap. (Max. Disp.)
  - In Wet: Max. Cap. = Cap. (26.4 N)
- Normalized Force = (Force(i)-26.4N)/26.4N
  - In both mediums Max. Force = Force (Max. Disp.) ≈ 440 N

For the tests with the dry sample, Fig. 5 shows that the capacitance maintains a linear increasing trend with displacement or strain, in both the extension and contraction stages of the experiment. Trend lines show similar slopes with a very good fit to the data. Fig. 6 shows the force vs. strain graph for the same experiment. The hysteresis loop, which is evident in the figure is caused by viscoelastic behavior of the rope. Some viscoplastic deformation is also evident as the strain did not return to its initial value at the end of the experiment. It is likely that repeated loading of the sample will "bed" the fibers and the viscoplastic behavior will no longer be visible.

An interesting, but expected, trend is seen for the same sample in the wet condition. Fig.7 shows a linear trend between the capacitance and strain, however it is a reverse of that observed in the dry. This is due to the change in material between the two wires and the respective dielectric constants as discussed earlier. When the rope is dry, the material between the wires is a mix of air and rope material, both of which have dielectric constants near 1. When the rope is submerged, the materials between the wires are rope and water. Notably, water has a dielectric constant close to 80. When tension is applied to the wet rope, the water is "squeezed" out and the overall

dielectric constant of the space between the wires decreases; trending towards that of the rope. The capacitance between a pair of wires is directly proportional to the dielectric constant of the material between them, causing the decreasing capacitance between the wires. This is due to the change in ratio of dielectric makeup between the two wires. Even though the wires are being drawn together with the tension, the dielectric constant of the mixture trends more heavily towards that of rope, not water. The force vs. strain curve shows a similar behavior as in the dry, with different values for the coefficients of the fitted curves, Fig. 8.

Trends across various samples were similar to those discussed above. At maximum load applied on different samples of the rope, Table 1 shows that the strain varies between 2.9% and 3.8% in dry and 1.89% and 2.95% in wet while the capacitance varies between 11.93% and 14.81% in dry and –43.48% and –57.28% in wet.

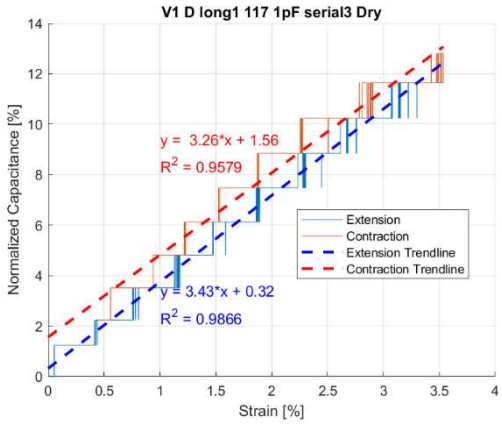

Figure 5. Normalized capacitance vs. Strain in the dry condition for one sample labeled V1D Long.

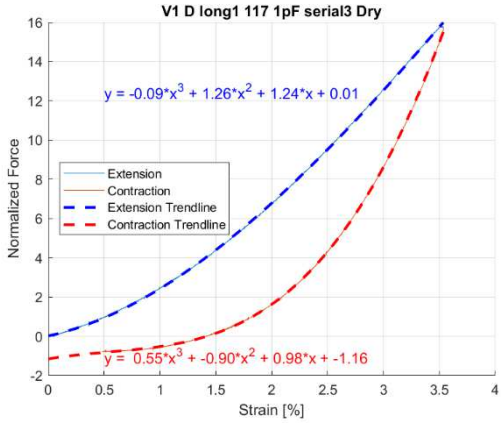

Figure 6. Normalized force vs. Strain in the dry condition for one sample labeled V1D Long. The hysteresis loop is clearly visible between the extension (blue) and contraction (Red) conditions.

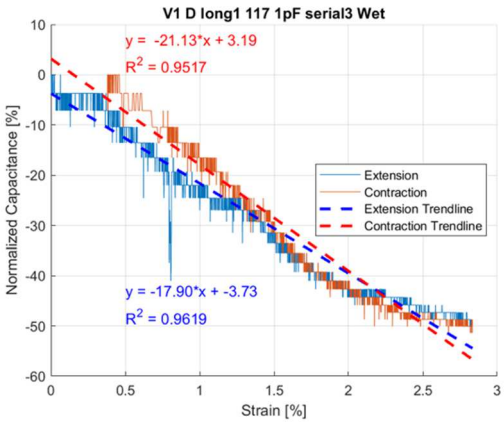

Figure 7. Normalized capacitance vs. Strain in the wet condition for one sample labeled V1D Long.

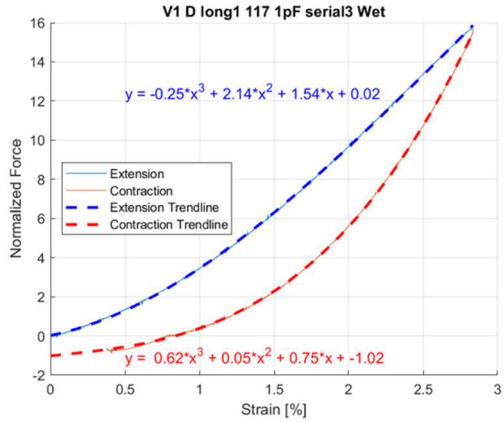

Figure 8. Normalized force vs. Strain in the wet condition for one sample labeled V1D Long. Similar to Fig. 6, the hysteresis loop is visible between the extension (blue) and contraction (Red) conditions.

Table 1. Normalized Force, Strain, and Normalized Capacitance at maximum displacement for the tested samples in dry and wet

		Norm. Force	Strain	Norm. Capacitance
			[%]	[%]
Dry	V1S Short	15.62	3.06	14.06
	V1D Short	15.66	3.8	11.93
	V1S Long	15.65	2.9	14.81
	V1D Long	15.65	3.54	13.36
Wet	V1S Short	15.64	1.89	-43.48
	V1D Short	15.67	2.95	-57.28
	V1S Long	15.7	2.66	-47.87
	V1D Long	15.7	2.83	-51.4

V. Conclusions

A sensor-integrated rope sample was tested in dry and wet conditions to measure changes in capacitance with elongation and relaxation. The observed linear trend of capacitance with strain offers strong potential for the sensor to support condition monitoring efforts of mooring lines for aquaculture and marine renewable energy. With further development, such a rope could be integrated into an aquaculture system to precisely locate excessive strains on a rope and means of developing advanced warning systems ahead of failures

Acknowledgment

The authors acknowledge the financial support of MIT Sea Grant to the University of Massachusetts Amherst through the United States Department of Commerce/ NOAA Award No. NA22OAR4170126 (Prime) CFDA NO. 11.417, Sea Grant Support. The authors acknowledge contributions from Dr. Kenneth Rolt (MITRE) on technical analysis for the capacitance model.

References

[1] FAO, *The State of World Fisheries and Aquaculture 2024*. FAO ;, 2024. Accessed: Jul. 20, 2024. [Online]. Available: https://openknowledge.fao.org/handle/20.500.14283/cd0683en

[2] S. Liu, Y. Sun, X. Jiang, and Y. Kang, "A Review of Wire Rope Detection Methods, Sensors and Signal Processing Techniques," *J. Nondestruct. Eval.*, vol. 39, no. 4, p. 85, Nov. 2020, doi: 10.1007/s10921-020-00732-y.

[3] T. Gordelier, P. R. Thies, G. Rinaldi, and L. Johanning, "Investigating Polymer Fibre Optics for Condition Monitoring of Synthetic Mooring Lines," *J. Mar. Sci. Eng.*, vol. 8, no. 2, Art. no. 2, Feb. 2020, doi: 10.3390/jmse8020103.

[4] C. R. Paul, *Analysis of Multiconductor Transmission Lines*. IEEE, 2007. doi: 10.1109/9780470547212.

[5] ABS, "Requirements for the Application of Fiber Rope for Offshore Mooring," American Bureau of Shipping, Houston, Texas, 2024.